# The Heteronuclear Cluster Chemistry of the Group 1B Metals. Part 7.[1] Synthesis and Gold-197 Mössbauer Spectra of the Mixed-metal Cluster Compounds $[Au_2Ru_4(\mu_3\text{-}H)(\mu\text{-}H)\{\mu\text{-}Ph_2E(CH_2)_nE'Ph_2\}(CO)_{12}]$ ($n$ = 1 or 2, E = E' = As or E = As, E' = P; $n$ = 2, E = E' = P). *X*-Ray Crystal Structure of $[Au_2Ru_4(\mu_3\text{-}H)(\mu\text{-}H)(\mu\text{-}Ph_2AsCH_2PPh_2)(CO)_{12}]$†

**Scott S. D. Brown and Ian D. Salter***
*Department of Chemistry, University of Exeter, Exeter EX4 4QD*
**David B. Dyson and R. V. ('Dick') Parish***
*Department of Chemistry, The University of Manchester Institute of Science and Technology, Manchester M60 1QD*
**Paul A. Bates and Michael B. Hursthouse**
*Department of Chemistry, Queen Mary College, University of London, London E1 4NS*

Treatment of acetone solutions of the salt $[N(PPh_3)_2]_2[Ru_4(\mu\text{-}H)_2(CO)_{12}]$ with a dichloromethane solution of the appropriate complex $[Au_2\{\mu\text{-}Ph_2E(CH_2)_nE'Ph_2\}Cl_2]$, in the presence of $TlPF_6$, affords the mixed-metal cluster compounds $[Au_2Ru_4(\mu_3\text{-}H)(\mu\text{-}H)\{\mu\text{-}Ph_2E(CH_2)_nE'Ph_2\}(CO)_{12}]$ [E = E' = P, $n$ = 2 (**3**); E = E' = As, $n$ = 1 (**4**) or 2 (**5**); E = As, E' = P, $n$ = 1 (**6**) or 2 (**7**)] in *ca.* 50—70% yield. An *X*-ray diffraction study on $[Au_2Ru_4(\mu_3\text{-}H)(\mu\text{-}H)(\mu\text{-}Ph_2AsCH_2PPh_2)(CO)_{12}]$ (**6**) revealed a metal-core structure consisting of a square-based pyramid, defined by two Au atoms and two Ru atoms in the basal plane and a Ru atom at the apex, with the $Ru_3$ face of this $Au_2Ru_3$ unit capped by a Ru atom [Au–Au 2.832(4), Au–Ru 2.689(4)—2.846(4), and Ru–Ru 2.792(5)—3.029(5) Å]. The asymmetrical bidentate ligand bridges the two Au atoms, one hydrido ligand caps a $Ru_3$ face and one bridges a Ru–Ru edge of the metal framework, and each Ru atom is ligated by three terminal CO groups. The $^{197}$Au Mössbauer spectra of clusters (**3**)—(**7**) are reported. These data suggest that $[Au_2Ru_4(\mu_3\text{-}H)(\mu\text{-}H)(\mu\text{-}Ph_2AsCH_2AsPh_2)(CO)_{12}]$ (**4**) exhibits a similar skeletal geometry to that of (**6**), whereas (**3**), (**5**), and (**7**) all adopt a capped trigonal-bipyramidal metal-core structure, with the two gold atoms occupying geometrically distinct sites.

Mössbauer spectra, using $^{197}$Au, have been reported for many homonuclear clusters of gold.[2,3] However, the technique has proved to be relatively insensitive to the number of Au–Au contacts and it cannot normally resolve signals from gold atoms which occupy geometrically non-equivalent sites and bear the same external ligands. Recently, however, we have demonstrated[4] that the more marked differences between the gold sites in heteronuclear clusters make their spectra more sensitive to structural effects and that Mössbauer spectroscopy can provide important information about the ground-state skeletal geometries adopted by these species. For example, the technique can easily detect the change in metal framework geometry which occurs when two $PPh_3$ groups attached to the gold atoms in $[Au_2Ru_4(\mu_3\text{-}H)(\mu\text{-}H)(CO)_{12}(PPh_3)_2]$ (**1**)[5] are formally replaced by a $Ph_2PCH_2PPh_2$ ligand in $[Au_2Ru_4(\mu_3\text{-}H)(\mu\text{-}H)(\mu\text{-}Ph_2PCH_2PPh_2)(CO)_{12}]$ (**2**).[6] The $^{197}$Au Mössbauer spectrum of (**1**) shows a signal for each of the two geometrically distinct gold sites within the capped trigonal-bipyramidal cluster skeleton.[4] However, only one signal is observed for (**2**), which adopts a capped square-based pyramidal metal framework structure, in which the two gold atoms are equivalent except for the position of one of the hydrido ligands.[4] In view of these interesting results, we decided to synthesize a series of clusters analogous to (**2**) in which the gold atoms are ligated by $Ph_2E(CH_2)_nE'Ph_2$ ($n$ = 2, E = E' = P; $n$ = 1 or 2, E = E' = As or E = As, E' = P) and to study the effect of the changes in ligand on the metal framework geometries and the Mössbauer spectra of these species.

## Results and Discussion

A solution of the complex $[Au_2\{\mu\text{-}Ph_2E(CH_2)_nE'Ph_2\}Cl_2]$ was prepared by treating a dichloromethane solution containing 2 equivalents of $[AuCl(SC_4H_8)]$ with 1 equivalent of the appropriate bidentate ligand. The addition of an acetone solution of the salt $[N(PPh_3)_2]_2[Ru_4(\mu\text{-}H)_2(CO)_{12}]$,[7] together with solid $TlPF_6$, to the resultant solution afforded, after working up, 50—70% yields of the dark red mixed-metal cluster compounds $[Au_2Ru_4(\mu_3\text{-}H)(\mu\text{-}H)\{\mu\text{-}Ph_2E(CH_2)_nE'Ph_2\}(CO)_{12}]$ [E = E' = P, $n$ = 2 (**3**); E = E' = As, $n$ = 1 (**4**) or 2 (**5**); E = As, E' = P, $n$ = 1 (**6**) or 2 (**7**)]. The microanalyses and i.r. and n.m.r. spectroscopic data for (**3**)—(**7**) (Tables 1 and 2) are all consistent with the proposed formulations and these species were also characterized by $^{197}$Au Mössbauer spectroscopy (Table 3).

The $^{197}$Au Mössbauer spectrum of the $Ph_2P(CH_2)_2PPh_2$-containing cluster (**3**) (Figure 1) consists of two overlapping doublets with very similar isomer shift (i.s.) and quadrupole splitting (q.s.) values to those previously reported[4] for the analogous $PPh_3$-ligated cluster (**1**). Thus, it seems likely that (**3**) adopts a similar capped trigonal-bipyramidal metal-core structure to that of (**1**).[5] This hypothesis is supported by the $^1$H and $^{31}$P-{$^1$H} n.m.r. spectra of (**3**). The data closely resemble those reported for (**1**)[5] and are in marked contrast to those observed for the $Ph_2PCH_2PPh_2$-containing cluster (**2**), which adopts a capped square-based pyramidal skeletal geometry.[6] At ambient temperature in solution, (**1**) undergoes a fluxional process which exchanges the gold atoms and the attached phosphorus atoms between the two inequivalent sites in the metal

† $\mu_3$-{$\mu$-[Diphenylarsino(diphenylphosphino)methane-*As*(Au)*P*(Au')]-diaurio(*Au–Au*)-*Au*(Ru$^{1,2}$)*Au'*(Ru$^{1,3}$)}-2,3-$\mu$-hydrido-1,2,4-$\mu_3$-hydrido-*cyclo*-tetrakis(tricarbonylruthenium)(4*Au–Ru*, 6*Ru–Ru*).

*Supplementary data available:* see Instructions for Authors, *J. Chem. Soc., Dalton Trans.*, 1988, Issue 1, pp. xvii—xx.

**Table 1.** Analytical[a] and physical data for the new gold heteronuclear cluster compounds

| Compound | M.p. (decomp.)/°C | $\nu_{max.}$(CO)[b]/cm$^{-1}$ | Yield (%)[c] | Analysis C | Analysis H |
|---|---|---|---|---|---|
| (3) $[Au_2Ru_4(\mu_3\text{-}H)(\mu\text{-}H)\{\mu\text{-}Ph_2P(CH_2)_2PPh_2\}(CO)_{12}]$ | 134—138 | 2 068s, 2 038s, 2 017vs, 1 974m(br), 1 935w(br) | 60 | 29.5 (29.7) | 1.5 (1.7) |
| (4) $[Au_2Ru_4(\mu_3\text{-}H)(\mu\text{-}H)(\mu\text{-}Ph_2AsCH_2AsPh_2)(CO)_{12}]$ | 140—145 | 2 075s, 2 046s, 2 024vs, 1 978m(br), 1 930w(br) | 52 | 27.8 (27.6) | 1.8 (1.5) |
| (5) $[Au_2Ru_4(\mu_3\text{-}H)(\mu\text{-}H)\{\mu\text{-}Ph_2As(CH_2)_2AsPh_2\}(CO)_{12}]$ | 125—130 | 2 074s, 2 044s, 2 021vs, 1 978m(br), 1 934w(br) | 70 | 28.0 (28.1) | 1.6 (1.6) |
| (6) $[Au_2Ru_4(\mu_3\text{-}H)(\mu\text{-}H)(\mu\text{-}Ph_2AsCH_2PPh_2)(CO)_{12}]$ | 144—146 | 2 075s, 2 045s, 2 023vs, 1 978m(br), 1 930w(br) | 55 | 28.4 (28.4) | 1.6 (1.5) |
| (7) $[Au_2Ru_4(\mu_3\text{-}H)(\mu\text{-}H)\{\mu\text{-}Ph_2As(CH_2)_2PPh_2\}(CO)_{12}]$ | 145—148 | 2 072s, 2 043s, 2 020vs, 1 976m(br), 1 937w(br) | 59 | 28.9 (28.9) | 1.8 (1.6) |

[a] Calculated values are given in parentheses. [b] Measured in dichloromethane solution. [c] Based on ruthenium reactant.

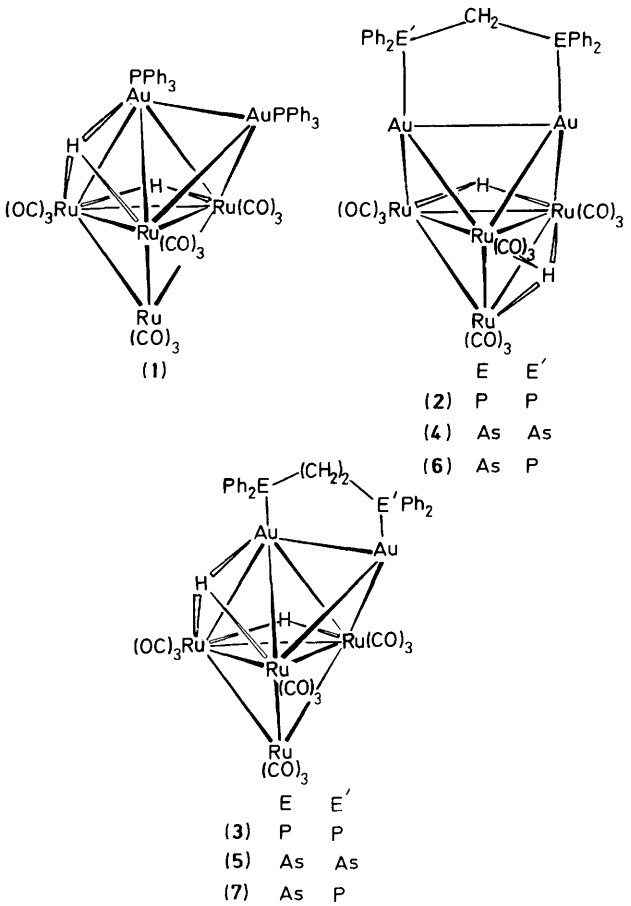


skeleton.[5] The room-temperature $^1H$ and $^{31}P\text{-}\{^1H\}$ n.m.r. spectra of (3) both show a single averaged phosphorus environment, thus (3) must undergo a similar intramolecular metal-core rearrangement, even though the two gold atoms are linked together by the bidentate diphosphine ligand. This type of dynamic behaviour has also been previously observed for analogous clusters in which two copper or silver atoms are ligated by $Ph_2P(CH_2)_nPPh_2$ ($n$ = 1—6).[1,8] As observed for (1),[5] spectra consistent with the ground state of (3) cannot be obtained, even at −90 °C, although both the high-field $^1H$ n.m.r. hydrido ligand peak and the $^{31}P\text{-}\{^1H\}$ n.m.r. signal show considerable broadening at this temperature. The similarity of the $^1H$ n.m.r. data to those reported[5] for (1) suggests that the hydrido ligands in (3) adopt the same positions as those in (1)

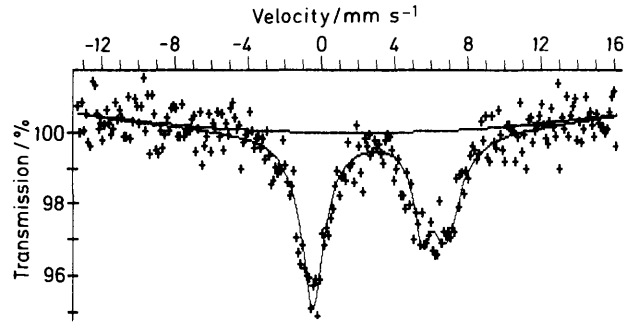


**Figure 1.** $^{197}$Au Mössbauer spectrum of $[Au_2Ru_4(\mu_3\text{-}H)(\mu\text{-}H)\{\mu\text{-}Ph_2P(CH_2)_2PPh_2\}(CO)_{12}]$ (3)

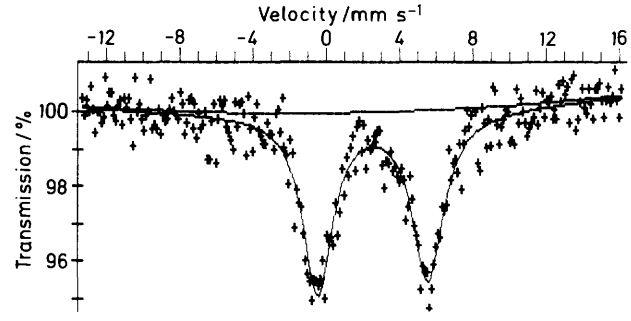


**Figure 2.** $^{197}$Au Mössbauer spectrum of $[Au_2Ru_4(\mu_3\text{-}H)(\mu\text{-}H)(\mu\text{-}Ph_2AsCH_2AsPh_2)(CO)_{12}]$ (4)

and that they undergo similar dynamic behaviour involving site-exchange at ambient temperature in solution.

The $^{197}$Au Mössbauer spectra of the clusters (4) and (5), which contain $Ph_2As(CH_2)_nAsPh_2$ ($n$ = 1 or 2), show that each of these species exhibits a similar metal-core structure to its $Ph_2P(CH_2)_nPPh_2$ analogue [(2)[6] and (3), respectively]. The spectrum of (4) (Figure 2) consists of a single signal, suggesting that (4) adopts a capped square-based pyramidal skeletal geometry. Both the i.s. and q.s. values decrease when the P atoms attached to gold are replaced by As atoms, which is also the trend observed for monomeric gold complexes.[9] In contrast to that of (4), the $^{197}$Au Mössbauer spectrum of (5) clearly shows two overlapping signals due to the two geometrically inequivalent gold sites in a capped trigonal-bipyramidal metal framework. As observed for its $Ph_2P(CH_2)_2PPh_2$-containing analogue (3), only a single methylene resonance is visible in the room-temperature $^1H$ n.m.r. spectrum of (5), suggesting that (5)

undergoes a similar intramolecular metal-core rearrangement to that of (3) in solution at this temperature. The high-field $^1H$ n.m.r. hydrido ligand signals for (4) and (5) are both singlets at ambient temperature, but they broaden on cooling until they are too broad to be visible at −90 °C. The data imply that the hydrido ligands in both clusters adopt inequivalent ground-state positions and undergo dynamic behaviour involving site-exchange at ambient temperature in solution. These observations are consistent with the hydrido ligands in (4) and (5) occupying the same positions as those in (2) and (1), respectively, and similar hydrido ligand dynamic behaviour has been observed for both of the latter species.[5,6]

To aid the interpretation of the $^{197}Au$ Mössbauer and n.m.r. spectroscopic data for the clusters (6) and (7), which contain the asymmetrical bidentate ligands $Ph_2As(CH_2)_nPPh_2$ ($n$ = 1 or 2), a single-crystal $X$-ray diffraction study was performed on (6).

**Table 2.** Hydrogen-1 and phosphorus-31 data[a] for the new gold heteronuclear cluster compounds

| Cluster | θ$_c$/°C | $^1H$[b] | $^{31}P$-{$^1H$}[c] |
|---|---|---|---|
| (3) | Ambient | [d] −16.18 [t, 2 H, hydrido H, $J$(PH) 5], 2.77 [AA′X pattern, 4 H, $PCH_2CH_2P$, $N$(PH) 13], 7.49—7.53 (m, 20 H, Ph) | 61.1 (s) |
| | −90 °C | *ca.* −16 (s vbr, 2 H) | *ca.* 58 (s vbr) |
| (4) | Ambient[e] | −17.09 (s, 2 H, hydrido H), 3.44 (s, 2 H, $AsCH_2As$), 7.29—7.51 (m, 20 H, Ph) | — |
| (5) | Ambient[e] | −16.85 (s, 2 H, hydrido H), 2.93 (s, 4 H, $AsCH_2CH_2As$), 7.46—7.63 (m, 20 H, Ph) | — |
| (6) | Ambient | −17.03 [d, 2 H, hydrido H, $J$(PH) 2], 3.61 [d, 2 H, $AsCH_2P$, $J$(PH) 10], 7.30—7.52 (m, 20 H, Ph) | 52.0 (s) |
| | −90 °C | No hydrido H signal visible | 49.2 (s br) |
| (7) | Ambient | −16.58 [d, 2 H, hydrido H, $J$(PH) 2], 2.68—3.00 (m, 4 H, $AsCH_2CH_2P$), 7.48—7.70 (m, 20 H, Ph) | 60.2 (s) |
| | −90 °C | No hydrido H signal visible | 57.7 (s br) |

[a] Chemical shifts (δ) in p.p.m., coupling constants in Hz. [b] Measured in [$^2H_2$]dichloromethane solution. At −90 °C, only the data for the hydrido ligands are presented. [c] Hydrogen-1 decoupled, measured in [$^2H_2$]dichloromethane solution, chemical shifts positive to high frequency of 85% $H_3PO_4$ (external). [d] $N$(PH) = |$J$(PH) + $J$(P′H)|. [e] No hydrido H signal visible at −90 °C.

**Table 3.** $^{197}Au$ Mössbauer data (mm s$^{-1}$) for the gold heteronuclear clusters $[Au_2Ru_4(\mu_3\text{-}H)(\mu\text{-}H)L_2(CO)_{12}]$, with the parameters of some mononuclear gold complexes for comparison

| Compound | I.s. (Au) | Q.s. | Linewidth |
|---|---|---|---|
| (2)[a] $L_2$ = $Ph_2PCH_2PPh_2$ | 3.02 | 6.71 | 1.90, 1.98 |
| (6) $L_2$ = $Ph_2AsCH_2PPh_2$ | 2.9[b] | 7.1 | 1.9 |
| | 2.5[c] | 5.5 | 1.6 |
| (4) $L_2$ = $Ph_2AsCH_2AsPh_2$ | 2.53 | 5.93 | 1.94, 2.06 |
| (1)[a] $L_2$ = $2PPh_3$ | 2.3 | 5.4 | 2.2 |
| | 3.0 | 7.5 | 1.8 |
| (3) $L_2$ = $Ph_2P(CH_2)_2PPh_2$ | 2.5 | 5.8 | 1.9 |
| | 3.1 | 7.2 | 2.0 |
| (7) $L_2$ = $Ph_2As(CH_2)_2PPh_2$ | 2.2[c] | 5.3 | 2.1 |
| | 2.6[b] | 7.0 | 2.0 |
| (5) $L_2$ = $Ph_2As(CH_2)_2AsPh_2$ | 2.3 | 5.1 | 2.2 |
| | 2.4 | 6.6 | 1.6 |
| $[AuCl(PPh_3)]$[d] | 4.08 | 7.43 | |
| $[AuCl(AsPh_3)]$[d] | 3.08 | 6.96 | |
| $[AuCl(PMe_2Ph)]$[d] | 3.91 | 7.11 | |
| $[AuCl(AsMe_2Ph)]$[d] | 2.93 | 6.37 | |

[a] Ref. 4. [b] Signal due to gold atom bonded to phosphorus. [c] Signal due to gold atom bonded to arsenic. [d] Ref. 9.

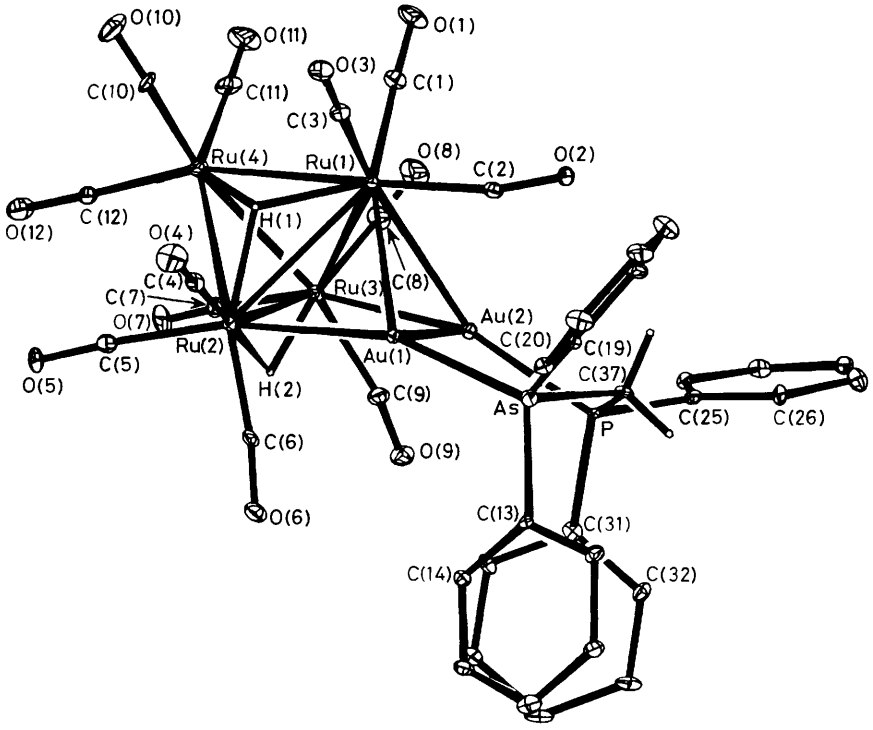


**Figure 3.** Molecular structure of $[Au_2Ru_4(\mu_3\text{-}H)(\mu\text{-}H)(\mu\text{-}Ph_2AsCH_2PPh_2)(CO)_{12}]$ (6), showing the atomic numbering scheme

**Table 4.** Bond lengths (Å) and angles (°), with estimated standard deviations in parentheses, for $[Au_2Ru_4(\mu_3\text{-}H)(\mu\text{-}H)(\mu\text{-}Ph_2AsCH_2PPh_2)(CO)_{12}]$ (**6**)

| | | | | | | | |
|---|---|---|---|---|---|---|---|
| Au(2)–Au(1) | 2.832(4) | C(4)–O(4) | 1.129(26) | Ru(1)–Au(1) | 2.821(4) | C(5)–O(5) | 1.119(24) |
| Ru(2)–Au(1) | 2.715(4) | C(6)–O(6) | 1.158(22) | As–Au(1) | 2.421(4) | C(7)–O(7) | 1.139(24) |
| Ru(1)–Au(2) | 2.846(4) | C(8)–O(8) | 1.101(29) | Ru(3)–Au(2) | 2.689(4) | C(9)–O(9) | 1.136(27) |
| P–Au(2) | 2.309(5) | C(10)–O(10) | 1.143(29) | Ru(2)–Ru(1) | 3.029(5) | C(11)–O(11) | 1.100(27) |
| Ru(3)–Ru(1) | 2.969(5) | C(12)–O(12) | 1.125(25) | Ru(4)–Ru(1) | 2.871(5) | C(14)–C(13) | 1.382(20) |
| C(1)–Ru(1) | 1.901(18) | C(18)–C(13) | 1.400(21) | C(2)–Ru(1) | 1.890(20) | C(15)–C(14) | 1.361(23) |
| C(3)–Ru(1) | 1.870(20) | C(16)–C(15) | 1.384(29) | Ru(3)–Ru(2) | 3.029(5) | C(17)–C(16) | 1.369(29) |
| Ru(4)–Ru(2) | 2.902(5) | C(18)–C(17) | 1.434(26) | C(4)–Ru(2) | 1.908(21) | C(20)–C(19) | 1.341(22) |
| C(5)–Ru(2) | 1.925(20) | C(24)–C(19) | 1.429(22) | C(6)–Ru(2) | 1.869(18) | C(21)–C(20) | 1.426(26) |
| Ru(4)–Ru(3) | 2.792(5) | C(22)–C(21) | 1.356(27) | C(7)–Ru(3) | 1.890(21) | C(23)–C(22) | 1.358(29) |
| C(8)–Ru(3) | 1.879(24) | C(24)–C(23) | 1.388(28) | C(9)–Ru(3) | 1.940(24) | C(26)–C(25) | 1.399(23) |
| C(10)–Ru(4) | 1.879(23) | C(30)–C(25) | 1.408(22) | C(11)–Ru(4) | 1.907(22) | C(27)–C(26) | 1.421(26) |
| C(12)–Ru(4) | 1.862(20) | C(28)–C(27) | 1.395(29) | C(13)–As | 1.943(15) | C(29)–C(28) | 1.382(27) |
| C(19)–As | 1.905(17) | C(30)–C(29) | 1.374(23) | C(37)–As | 1.955(16) | C(32)–C(31) | 1.402(23) |
| C(25)–P | 1.816(16) | C(36)–C(31) | 1.389(22) | C(31)–P | 1.813(17) | C(33)–C(32) | 1.369(26) |
| C(37)–P | 1.827(15) | C(34)–C(33) | 1.443(28) | C(1)–O(1) | 1.113(22) | C(35)–C(34) | 1.355(29) |
| C(2)–O(2) | 1.148(23) | C(36)–C(35) | 1.385(22) | C(3)–O(3) | 1.140(26) | | |
| | | | | | | | |
| Ru(1)–Au(1)–Au(2) | 60.5(2) | C(19)–As–Au(1) | 119.0(6) | Ru(2)–Au(1)–Au(2) | 87.5(2) | C(19)–As–C(13) | 103.1(7) |
| Ru(2)–Au(1)–Ru(1) | 66.3(2) | C(37)–As–Au(1) | 107.9(5) | As–Au(1)–Au(2) | 95.3(2) | C(37)–As–C(13) | 101.5(6) |
| As–Au(1)–Ru(1) | 131.2(1) | C(37)–As–C(19) | 102.7(7) | As–Au(1)–Ru(2) | 160.7(1) | C(25)–P–Au(2) | 115.4(6) |
| Ru(1)–Au(2)–Au(1) | 59.6(2) | C(31)–P–Au(2) | 113.8(6) | Ru(3)–Au(2)–Au(1) | 96.2(2) | C(31)–P–C(25) | 104.6(8) |
| Ru(3)–Au(2)–Ru(1) | 64.8(2) | C(37)–P–Au(2) | 112.8(6) | P–Au(2)–Au(1) | 92.0(2) | C(37)–P–C(25) | 104.6(7) |
| P–Au(2)–Ru(1) | 136.4(1) | C(37)–P–C(31) | 104.5(7) | P–Au(2)–Ru(3) | 157.5(1) | O(1)–C(1)–Ru(1) | 174.9(14) |
| Au(2)–Ru(1)–Au(1) | 60.0(2) | O(2)–C(2)–Ru(1) | 165.8(15) | Ru(2)–Ru(1)–Au(1) | 55.2(2) | O(3)–C(3)–Ru(1) | 179.0(16) |
| Ru(2)–Ru(1)–Au(2) | 81.5(2) | O(4)–C(4)–Ru(2) | 177.7(17) | Ru(3)–Ru(1)–Au(1) | 90.4(2) | O(5)–C(5)–Ru(2) | 175.4(16) |
| Ru(3)–Ru(1)–Au(2) | 55.0(2) | O(6)–C(6)–Ru(2) | 171.6(14) | Ru(3)–Ru(1)–Ru(2) | 60.7(2) | O(7)–C(7)–Ru(3) | 172.6(18) |
| Ru(4)–Ru(1)–Au(1) | 114.0(2) | O(8)–C(8)–Ru(3) | 178.0(20) | Ru(4)–Ru(1)–Au(2) | 111.6(2) | O(9)–C(9)–Ru(3) | 166.0(16) |
| Ru(4)–Ru(1)–Ru(2) | 58.8(2) | O(10)–C(10)–Ru(4) | 177.2(18) | Ru(4)–Ru(1)–Ru(3) | 57.1(2) | O(11)–C(11)–Ru(4) | 177.6(18) |
| C(1)–Ru(1)–Au(1) | 163.0(6) | O(12)–C(12)–Ru(4) | 177.1(17) | C(1)–Ru(1)–Au(2) | 109.8(8) | C(14)–C(13)–As | 118.7(11) |
| C(1)–Ru(1)–Ru(2) | 140.2(5) | C(18)–C(13)–As | 119.6(11) | C(1)–Ru(1)–Ru(3) | 93.8(6) | C(18)–C(13)–C(14) | 121.7(14) |
| C(1)–Ru(1)–Ru(4) | 81.9(6) | C(15)–C(14)–C(13) | 120.1(15) | C(2)–Ru(1)–Au(1) | 71.0(6) | C(16)–C(15)–C(14) | 121.2(17) |
| C(2)–Ru(1)–Au(2) | 64.6(7) | C(17)–C(16)–C(15) | 119.3(19) | C(2)–Ru(1)–Ru(2) | 125.7(6) | C(18)–C(17)–C(16) | 121.7(19) |
| C(2)–Ru(1)–Ru(3) | 117.6(7) | C(17)–C(18)–C(13) | 116.1(16) | C(2)–Ru(1)–Ru(4) | 171.8(6) | C(20)–C(19)–As | 120.0(12) |
| C(2)–Ru(1)–C(1) | 92.5(8) | C(24)–C(19)–As | 121.0(13) | C(3)–Ru(1)–Au(1) | 92.3(6) | C(24)–C(19)–C(20) | 119.0(16) |
| C(3)–Ru(1)–Au(2) | 147.8(5) | C(21)–C(20)–C(19) | 118.7(17) | C(3)–Ru(1)–Ru(2) | 96.4(6) | C(22)–C(21)–C(20) | 122.7(19) |
| C(3)–Ru(1)–Ru(3) | 149.0(5) | C(23)–C(22)–C(21) | 118.6(19) | C(3)–Ru(1)–Ru(4) | 94.0(7) | C(24)–C(23)–C(22) | 120.7(18) |
| C(3)–Ru(1)–C(1) | 92.5(9) | C(23)–C(24)–C(19) | 120.2(17) | C(3)–Ru(1)–C(2) | 92.3(9) | C(26)–C(25)–P | 123.7(12) |
| Ru(1)–Ru(2)–Au(1) | 58.5(2) | C(30)–C(25)–P | 117.8(12) | Ru(3)–Ru(2)–Au(1) | 91.2(2) | C(30)–C(25)–C(26) | 118.4(14) |
| Ru(3)–Ru(2)–Ru(1) | 58.7(2) | C(27)–C(26)–C(25) | 121.4(16) | Ru(4)–Ru(2)–Au(1) | 116.4(2) | C(28)–C(27)–C(26) | 117.5(18) |
| Ru(4)–Ru(2)–Ru(1) | 57.9(2) | C(29)–C(28)–C(27) | 121.5(18) | Ru(4)–Ru(2)–Ru(3) | 56.1(2) | C(30)–C(29)–C(28) | 120.4(17) |
| C(4)–Ru(2)–Au(1) | 82.4(7) | C(29)–C(30)–C(25) | 120.7(15) | C(4)–Ru(2)–Ru(1) | 95.0(6) | C(32)–C(31)–P | 121.3(13) |
| C(4)–Ru(2)–Ru(3) | 151.5(5) | C(36)–C(31)–P | 119.8(12) | C(4)–Ru(2)–Ru(4) | 102.2(6) | C(36)–C(31)–C(32) | 118.9(15) |
| C(5)–Ru(2)–Au(1) | 164.4(5) | C(33)–C(32)–C(31) | 122.0(17) | C(5)–Ru(2)–Ru(1) | 136.9(5) | C(34)–C(33)–C(32) | 118.0(19) |
| C(5)–Ru(2)–Ru(3) | 99.7(7) | C(35)–C(34)–C(33) | 119.5(18) | C(5)–Ru(2)–Ru(4) | 79.1(6) | C(36)–C(35)–C(34) | 121.9(17) |
| C(5)–Ru(2)–C(4) | 92.8(9) | C(35)–C(36)–C(31) | 119.6(16) | C(6)–Ru(2)–Au(1) | 69.1(6) | P–C(37)–As | 113.5(8) |
| C(6)–Ru(2)–Ru(1) | 125.4(6) | H(1)–Ru(1)–Au(1) | 82.1(2) | C(6)–Ru(2)–Ru(3) | 111.3(7) | H(1)–Ru(1)–Au(2) | 112.2(2) |
| C(6)–Ru(2)–Ru(4) | 165.0(6) | H(1)–Ru(1)–Ru(2) | 32.7(1) | C(6)–Ru(2)–C(4) | 92.3(9) | H(1)–Ru(1)–Ru(3) | 73.4(2) |
| C(6)–Ru(2)–C(5) | 96.4(8) | H(1)–Ru(1)–Ru(4) | 37.1(1) | Ru(1)–Ru(3)–Au(2) | 60.2(2) | H(1)–Ru(1)–C(1) | 114.9(7) |
| Ru(2)–Ru(3)–Au(2) | 84.1(2) | H(1)–Ru(1)–C(2) | 150.5(5) | Ru(2)–Ru(3)–Ru(1) | 60.7(2) | H(1)–Ru(1)–C(3) | 76.4(6) |
| Ru(4)–Ru(3)–Au(2) | 119.2(2) | H(1)–Ru(2)–Au(1) | 85.3(2) | Ru(4)–Ru(3)–Ru(1) | 59.7(2) | H(1)–Ru(2)–Ru(1) | 32.7(1) |
| Ru(4)–Ru(3)–Ru(2) | 59.6(2) | H(1)–Ru(2)–Ru(3) | 71.8(2) | C(7)–Ru(3)–Au(2) | 159.8(6) | H(1)–Ru(2)–Ru(4) | 36.3(1) |
| C(7)–Ru(3)–Ru(1) | 139.2(6) | H(1)–Ru(2)–C(4) | 80.0(6) | C(7)–Ru(3)–Ru(2) | 101.1(7) | H(1)–Ru(2)–C(5) | 108.6(6) |
| C(7)–Ru(3)–Ru(4) | 79.5(7) | H(1)–Ru(2)–C(6) | 154.1(5) | C(8)–Ru(3)–Au(2) | 89.6(7) | H(2)–Ru(2)–Au(1) | 93.1(39) |
| C(8)–Ru(3)–Ru(1) | 89.4(8) | H(2)–Ru(2)–Ru(1) | 86.7(20) | C(8)–Ru(3)–Ru(2) | 148.4(7) | H(2)–Ru(2)–Ru(3) | 32.7(24) |
| C(8)–Ru(3)–Ru(4) | 97.9(9) | H(2)–Ru(2)–Ru(4) | 84.1(36) | C(8)–Ru(3)–C(7) | 95.5(9) | H(2)–Ru(2)–C(4) | 173.4(40) |
| C(9)–Ru(3)–Au(2) | 65.9(7) | H(2)–Ru(2)–C(5) | 90.2(35) | C(9)–Ru(3)–Ru(1) | 126.0(7) | H(2)–Ru(2)–C(6) | 81.5(35) |
| C(9)–Ru(3)–Ru(2) | 113.4(7) | H(2)–Ru(2)–H(1) | 104.5(24) | C(9)–Ru(3)–Ru(4) | 169.0(6) | H(2)–Ru(3)–Au(2) | 83.0(39) |
| C(9)–Ru(3)–C(7) | 94.4(9) | H(2)–Ru(3)–Ru(1) | 88.6(33) | C(9)–Ru(3)–C(8) | 91.7(11) | H(2)–Ru(3)–Ru(2) | 32.7(25) |
| Ru(2)–Ru(4)–Ru(1) | 63.3(2) | H(2)–Ru(3)–Ru(4) | 87.5(27) | Ru(3)–Ru(4)–Ru(1) | 63.2(2) | H(2)–Ru(3)–C(7) | 90.9(40) |
| Ru(3)–Ru(4)–Ru(2) | 64.2(2) | H(2)–Ru(3)–C(8) | 172.3(37) | C(10)–Ru(4)–Ru(1) | 99.4(7) | H(2)–Ru(3)–C(9) | 83.5(27) |
| C(10)–Ru(4)–Ru(2) | 106.0(7) | H(1)–Ru(4)–Ru(1) | 37.1(1) | C(10)–Ru(4)–Ru(3) | 162.3(6) | H(1)–Ru(4)–Ru(2) | 36.3(1) |
| C(11)–Ru(4)–Ru(1) | 98.8(7) | H(1)–Ru(4)–Ru(3) | 78.3(2) | C(11)–Ru(4)–Ru(2) | 153.4(7) | H(1)–Ru(4)–C(10) | 85.5(7) |
| C(11)–Ru(4)–Ru(3) | 90.6(8) | H(1)–Ru(4)–C(11) | 134.6(6) | C(11)–Ru(4)–C(10) | 95.9(11) | H(1)–Ru(4)–C(12) | 131.8(6) |
| C(12)–Ru(4)–Ru(1) | 162.5(6) | Ru(2)–H(1)–Ru(1) | 114.6(2) | C(12)–Ru(4)–Ru(2) | 100.6(7) | Ru(4)–H(1)–Ru(1) | 105.8(2) |
| C(12)–Ru(4)–Ru(3) | 104.6(8) | Ru(4)–H(1)–Ru(2) | 107.4(2) | C(12)–Ru(4)–C(10) | 91.5(10) | Ru(3)–H(2)–Ru(2) | 114.6(36) |
| C(12)–Ru(4)–C(11) | 93.6(9) | | | C(13)–As–Au(1) | 120.0(5) | | |

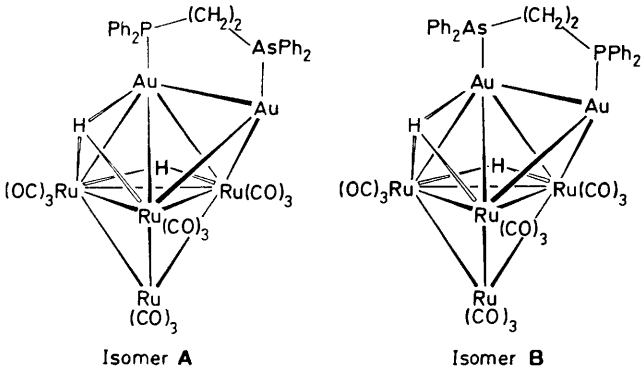


**Figure 4.** The two possible structural isomers of $[Au_2Ru_4(\mu_3\text{-}H)(\mu\text{-}H)\{\mu\text{-}Ph_2As(CH_2)_2PPh_2\}(CO)_{12}]$ (**7**)

The molecular structure of (**6**) is illustrated in Figure 3, which also shows the atomic numbering scheme. The interatomic distances and angles are summarized in Table 4. The molecular structure of (**6**) is isomorphous with that previously established for the analogous $Ph_2PCH_2PPh_2$-containing species (**2**).[6] The metal skeleton of (**6**) adopts a capped square-based pyramidal geometry, with the basal atoms Au(1), Au(2), Ru(2), and Ru(3) and the apical atom Ru(1) defining the square-based pyramid and Ru(4) capping its Ru(1)Ru(2)Ru(3) face. The asymmetrical $Ph_2AsCH_2PPh_2$ ligand bridges the Au–Au vector, with the As atom attached to Au(1) and the P atom to Au(2). The hydrido ligands were not located in the *X*-ray diffraction study, but they have been placed in the positions previously calculated for (**2**),[6] as (**6**) and (**2**) are isomorphous. Thus, one hydrido ligand occupies a site edge-bridging the Ru(2)–Ru(3) vector and the other has been placed in a position capping the Ru(1)Ru(2)Ru(4) face. Each ruthenium atom carries three terminal CO ligands and the Ru–C–O units are essentially linear.

The Au–Au separation in (**6**) [2.832(4) Å] is closely similar to that reported[6] for (**2**) [2.823(1) Å] and is somewhat longer than those observed for $[Au_2Ru_3(\mu_3\text{-}S)(\mu\text{-}Ph_2PCH_2PPh_2)(CO)_9]$ [2.802(1) Å][10] and $[Au_3Ru_4(\mu\text{-}H)(\mu\text{-}Ph_2PCH_2PPh_2)(CO)_{12}(PPh_3)]$ [2.758(2) Å].[11] The Au–Ru separations in (**6**) and (**2**) are little different, apart from the Au(2)–Ru(1) distance, which is *ca.* 0.1 Å shorter than the corresponding vector in (**2**). The Ru–Ru edges in (**6**) which are bridged by the Au atoms are between 0.02 and 0.04 Å longer than the equivalent separations in (**2**), but, within the error limits, the lengths of the unbridged Ru–Ru vectors in the two clusters are the same.

The Au–P bond length in (**6**) [2.309(5) Å] is identical to those reported[12] for (**2**) [2.304(3) and 2.309(3) Å], within the error limits, but the Au–As distance [2.421(4) Å] is significantly longer, as expected. The ruthenium carbonyl angles are in the normal range for terminal CO ligands (Ru–C–O *ca.* 166—179°). However, short Au–C distances are often observed for essentially linear carbonyl groups bonded to adjacent metals in gold heteronuclear clusters[10,13,14] and three such contacts occur in (**6**) [Au(1)···C(6) 2.69, Au(2)···C(2) 2.66, and Au(2)···C(9) 2.60 Å].

As expected, the $^{197}$Au Mössbauer spectra of clusters (**6**) and (**7**) both consist of two signals, one due to the gold atom attached to arsenic and the other due to the gold atom bonded to phosphorus. For the $Ph_2AsCH_2PPh_2$-containing species (**6**), the values of i.s. and q.s. for one signal are very similar to those reported for (**2**),[4] whereas the parameters for the other signal closely resemble the values observed for (**4**). At ambient temperature, the high-field $^1$H n.m.r. hydrido ligand signal for (**6**) consists of a single resonance, which broadens as the temperature is lowered until it becomes too broad to be visible at −90 °C. Thus, in solution, the two inequivalent hydrido ligands in (**6**) undergo dynamic behaviour involving site exchange, as observed for the structurally closely related clusters (**2**)[6] and (**4**). The single phosphorus signal in the $^{31}$P-{$^1$H} n.m.r. spectrum of (**6**) is also broadened at −90 °C, which implies that the ground-state positions adopted by the hydrido ligands create more than one structural isomer in solution at low temperature. It seems reasonable to suggest that there are two such isomers, differing only in the position of the triply bridging hydrido ligand, which could cap a $Ru_3$ face adjacent to the gold atom attached to arsenic [Ru(1)Ru(2)Ru(4)] or a $Ru_3$ face adjacent to the gold atom bonded to phosphorus [Ru(1)Ru(3)Ru(4)]. As clusters (**3**) and (**5**), which contain $Ph_2E(CH_2)_2EPh_2$ (E = As or P), both exhibit capped trigonal-bipyramidal skeletal geometries, it is not unreasonable to propose that (**7**) adopts a similar metal-core structure. When the two gold atoms are linked by the asymmetrical bidentate ligand, two distinct structural isomers (labelled **A** and **B** in Figure 4) are possible for this metal framework geometry.[15] Comparison of the $^{197}$Au Mössbauer data for (**7**) with those for (**1**),[4] (**3**), and (**5**) suggests that the As atom is bonded to the gold atom with the higher connectivity in (**7**). Thus, it seems that (**7**) adopts the structure of isomer **B** in the solid state, although it is extremely unlikely that Mössbauer spectroscopy would be capable of resolving the two sets of signals if a small proportion of the total number of molecules of (**7**) existed as isomer **A**. The high-field $^1$H n.m.r. hydrido ligand signal of (**7**) is a doublet [*J*(PH) 2 Hz]. Previous studies on closely related copper and silver species have shown that $^{31}$P–$^1$H coupling on the hydrido ligand peaks is only observed when the phosphorus atom occupies the position in isomer **A** and that the magnitudes of these couplings lie in the range 9—13 Hz.[1,5,15] The single hydrido ligand resonance and greatly reduced *J*(PH) value observed for (**7**) suggest that **B** is the predominant isomer in solution at ambient temperature, although a small proportion of isomer **A** also exists, and that the two isomers are being interconverted by a dynamic process. It seems reasonable to propose that the mechanism for this interconversion is an intramolecular metal-core rearrangement, in view of the fact that both (**3**) and (**5**) undergo a fluxional process which exchanges the gold atoms between the two inequivalent sites. Similar results have been previously reported for the analogous copper cluster $[Cu_2Ru_4(\mu_3\text{-}H)_2\{\mu\text{-}Ph_2As(CH_2)_2PPh_2\}(CO)_{12}]$, for which the high-field $^1$H n.m.r. hydrido ligand signal is a doublet [*J*(PH) 3 Hz] at room temperature.[15] At ambient temperature in solution, the copper cluster exists predominantly as structural isomer **B** and an intramolecular metal-core rearrangement is thought to interconvert isomers **A** and **B**.[15] In the case of the copper species, the $^{31}$P-{$^1$H} n.m.r. spectrum at −90 °C shows a signal due to each isomer, but the resonance for (**7**) is a considerably broadened singlet, suggesting a lower value of $\Delta G^{\ddagger}$ for the dynamic process in the gold cluster. This observation is consistent with previously reported trends in $\Delta G^{\ddagger}$ for skeletal rearrangements.[5,10]

## Experimental

All reactions and manipulations were performed under an atmosphere of dry oxygen-free nitrogen, using standard Schlenk-tube techniques.[16] Solvents were freshly distilled under nitrogen from the usual drying agents immediately before use. Light petroleum refers to that fraction of b.p. 40—60 °C. Established methods were used to prepare $[N(PPh_3)_2]_2[Ru_4(\mu\text{-}H)_2(CO)_{12}]$,[7] $[AuCl(SC_4H_8)]$,[17] and $Ph_2As(CH_2)_nPPh_2$ ($n$ = 1[18] or 2[19]). The ligands $Ph_2E(CH_2)_nEPh_2$ (E = P, $n$ = 2; E = As, $n$ = 1 or 2) were purchased from Strem Chemicals Inc. and used without further purification. Analytical and other physical data for the new cluster compounds are presented in Table 1, together with their i.r. spectra. The results of n.m.r. and $^{197}$Au

**Table 5.** Quantities of bidentate ligand used and product obtained and the chromatography conditions employed for synthesis of the clusters $[Au_2Ru_4(\mu_3\text{-}H)(\mu\text{-}H)\{\mu\text{-}Ph_2E(CH_2)_nE'Ph_2\}(CO)_{12}]$

| $n$ | E | E′ | Quantity (g, mmol) of $Ph_2E(CH_2)_nE'Ph_2$ used | Quantity (g) of product obtained | Proportions of the dichloromethane–light petroleum mixture used for elution[a] | Temperature for the chromatography[b] |
|---|---|---|---|---|---|---|
| 2 | P | P | 0.07, 0.18 | 0.15 | 1:4 | Ambient |
| 1 | As | As | 0.08, 0.17 | 0.14 | 1:3 | −20 °C |
| 2 | As | As | 0.08, 0.17 | 0.19 | 1:2 | −20 °C |
| 1 | As | P | 0.07, 0.17 | 0.14 | 2:3 | Ambient |
| 2 | As | P | 0.08, 0.17 | 0.16 | 2:3 | Ambient |

[a] The crude product was initially dissolved in the same solvent mixture as that used for elution. [b] The chromatography was performed on an alumina column (20 × 3 cm).

**Table 6.** Atomic positional parameters (fractional co-ordinates) ( × $10^4$) for $[Au_2Ru_4(\mu_3\text{-}H)(\mu\text{-}H)(\mu\text{-}Ph_2AsCH_2PPh_2)(CO)_{12}]$ (**6**), with estimated standard deviations in parentheses

| Atom | $x$ | $y$ | $z$ | Atom | $x$ | $y$ | $z$ |
|---|---|---|---|---|---|---|---|
| Au(1) | 3 645.0(4) | 3 737.8(4) | 2 432.5(3) | C(10) | 848(13) | 5 622(12) | 1 544(12) |
| Au(2) | 2 579.8(4) | 2 446.2(4) | 2 052.1(3) | C(11) | −130(11) | 4 283(15) | 1 202(13) |
| Ru(1) | 2 252(1) | 3 904(1) | 1 317(1) | C(12) | −146(12) | 4 974(13) | 2 699(11) |
| Ru(2) | 2 185(1) | 4 405(1) | 3 072(1) | C(13) | 5 649(8) | 2 746(8) | 3 316(8) |
| Ru(3) | 1 036(1) | 3 106(1) | 2 448(1) | C(14) | 5 203(10) | 2 767(9) | 4 046(9) |
| Ru(4) | 711(1) | 4 627(1) | 1 980(1) | C(15) | 5 607(13) | 2 525(12) | 4 735(9) |
| As | 5 029(1) | 3 050(1) | 2 338(1) | C(16) | 6 469(14) | 2 264(12) | 4 726(12) |
| P | 3 760(2) | 1 612(2) | 2 160(2) | C(17) | 6 914(13) | 2 233(10) | 4 007(11) |
| O(1) | 1 105(10) | 3 708(12) | −155(8) | C(18) | 6 519(11) | 2 484(10) | 3 263(10) |
| O(2) | 3 636(9) | 3 016(9) | 398(7) | C(19) | 5 942(10) | 3 460(9) | 1 676(8) |
| O(3) | 3 000(11) | 5 391(10) | 675(8) | C(20) | 6 539(9) | 3 943(9) | 1 994(10) |
| O(4) | 3 222(11) | 5 884(9) | 2 822(11) | C(21) | 7 205(13) | 4 253(12) | 1 480(11) |
| O(5) | 916(10) | 5 206(9) | 4 223(8) | C(22) | 7 254(13) | 4 086(12) | 679(11) |
| O(6) | 3 322(8) | 3 856(10) | 4 456(7) | C(23) | 6 629(14) | 3 622(12) | 350(11) |
| O(7) | −679(9) | 3 333(10) | 3 346(9) | C(24) | 5 985(12) | 3 286(11) | 831(10) |
| O(8) | 169(10) | 2 334(12) | 1 048(9) | C(25) | 3 674(10) | 731(8) | 1 569(8) |
| O(9) | 1 209(9) | 1 575(8) | 3 351(8) | C(26) | 4 386(11) | 388(9) | 1 170(9) |
| O(10) | 895(12) | 6 231(11) | 1 282(12) | C(27) | 4 278(12) | −294(12) | 702(11) |
| O(11) | −635(11) | 4 079(14) | 775(9) | C(28) | 3 431(14) | −601(11) | 644(11) |
| O(12) | −689(9) | 5 180(11) | 3 108(10) | C(29) | 2 728(12) | −275(9) | 1 050(9) |
| C(1) | 1 496(10) | 3 776(13) | 410(10) | C(30) | 2 835(10) | 398(9) | 1 479(8) |
| C(2) | 3 156(12) | 3 312(12) | 836(10) | C(31) | 3 970(9) | 1 286(9) | 3 184(9) |
| C(3) | 2 714(12) | 4 827(11) | 912(10) | C(32) | 4 600(10) | 715(10) | 3 347(10) |
| C(4) | 2 851(12) | 5 325(11) | 2 910(10) | C(33) | 4 772(13) | 468(14) | 4 118(10) |
| C(5) | 1 356(12) | 4 913(11) | 3 775(10) | C(34) | 4 269(13) | 802(13) | 4 771(11) |
| C(6) | 2 942(11) | 4 062(12) | 3 888(9) | C(35) | 3 639(12) | 1 332(12) | 4 602(9) |
| C(7) | −25(12) | 3 300(12) | 3 010(12) | C(36) | 3 493(9) | 1 597(10) | 3 823(8) |
| C(8) | 502(13) | 2 612(16) | 1 563(13) | C(37) | 4 797(9) | 2 049(8) | 1 837(7) |
| C(9) | 1 253(12) | 2 127(13) | 2 983(12) | | | | |

Mössbauer spectroscopic measurements are summarized in Tables 2 and 3, respectively.

Infrared spectra were recorded on a Perkin-Elmer 299B spectrophotometer. Hydrogen-1 and $^{31}P\text{-}\{^1H\}$ n.m.r. spectra were measured on a Brüker AM 250 spectrometer. Product separation by column chromatography was performed on B.D.H. alumina (Brockman activity II).

*Synthesis of the Compounds* $[Au_2Ru_4(\mu_3\text{-}H)(\mu\text{-}H)\{\mu\text{-}Ph_2E(CH_2)_nE'Ph_2\}(CO)_{12}]$ ($n$ = 1 *or* 2, E = E′ = As *or* E = As, E′ = P; $n$ = 2, E = E′ = P).—A dichloromethane (10 $cm^3$) solution of $[AuCl(SC_4H_8)]$ (0.11 g, 0.34 mmol) was treated with the appropriate amount (Table 5) of the desired bidentate ligand $Ph_2E(CH_2)_nE'Ph_2$ and the mixture was stirred for 15 min. An acetone (40 $cm^3$) solution of $[N(PPh_3)_2]_2[Ru_4(\mu\text{-}H)_2(CO)_{12}]$ (0.30 g, 0.17 mmol), together with solid $TlPF_6$ (0.46 g, 1.32 mmol), was then added and the mixture was stirred for 1 h. The solvent was removed under reduced pressure and the residue was extracted with dichloromethane–diethyl ether (1:4, 25-$cm^3$ portions), until the extracts were no longer coloured red. The combined extracts were then filtered through a Celite pad (*ca.* 1 × 3 cm). After removal of the solvent from the filtrate under reduced pressure, the crude residue was dissolved and chromatographed, using the appropriate conditions (Table 5). The chromatography afforded one red fraction, which, after removal of the solvent under reduced pressure and crystallization of the residue from dichloromethane–light petroleum, yielded dark red *microcrystals* of $[Au_2Ru_4(\mu_3\text{-}H)(\mu\text{-}H)\{\mu\text{-}Ph_2E(CH_2)_nE'Ph_2\}(CO)_{12}]$. Table 5 lists the amounts of product obtained.

$^{197}Au$ *Mössbauer Spectroscopy*.—The Mössbauer spectra were recorded as described previously,[4,20] with both the source and the sample immersed in liquid helium, using *ca.* 25 mg Au $cm^{-2}$. In computer fitting of the spectra consisting of two overlapped doublets, the lines were constrained in pairs. The

estimated errors in i.s. and q.s. are *ca.* $\pm 0.05$ mm $s^{-1}$ in these cases.

*Crystal Structure Determination for Compound* (**6**).—Suitable crystals of cluster (**6**) were grown from a dichloromethane–light petroleum mixture by slow layer diffusion at −20 °C.

*Crystal data.* $C_{37}H_{24}AsAu_2O_{12}PRu_4$, $M = 1\,564.7$, orthorhombic, space group $P2_12_12_1$ (no. 19), $a = 15.187(4)$, $b = 17.326(3)$, $c = 16.525(3)$ Å, $U = 4\,348(1)$ Å$^3$, $Z = 4$, $D_c = 2.390$ g cm$^{-3}$, $F(000) = 2\,896$, $\lambda = 0.710\,69$ Å, $\mu$(Mo-$K_\alpha$) = 88.9 cm$^{-1}$.

The crystal used (0.43 × 0.38 × 0.30 mm) was sealed, under $N_2$, in a thin-walled glass capillary.

*Data collection.* Unit-cell parameters and intensity data were obtained by following previously detailed procedures,[21] using a CAD4 diffractometer operating in the ω–2θ scan mode, with graphite-monochromated Mo-$K_\alpha$ radiation. A total of 4 245 unique reflections were collected ($3 \leqslant 2\theta \leqslant 50°$). The segment of reciprocal space scanned was ($h$) 0 to 18, ($k$) 0 to 20, and ($l$) 0 to 19. The reflection intensities were corrected for absorption, using the azimuthal-scan method;[22] maximum transmission factor 1.00, minimum value 0.66.

*Structure solution and refinement.* The structure was solved by the application of routine heavy-atom methods (SHELX 86[23]), and refined by blocked-matrix least squares (SHELX 76[24]). All non-hydrogen atoms were refined anisotropically, and hydrogen atoms placed in calculated positions (C–H 0.96, Ru–H 1.80 Å;[25] $U = 0.10$ Å$^2$). The final residuals $R$ and $R'$ were 0.034 and 0.031, respectively, for the 521 variables and 3 322 data for which $F_o > 3\sigma(F_o)$. A test for the absolute configuration of the structure was made[24] ($R = 0.071$). The function minimized was $\Sigma w(|F_o| - |F_c|)^2$ with the weight, $w$, being defined as $1/[\sigma^2(F_o) + 0.0002F_o^2]$. Atomic scattering factors and anomalous scattering parameters were taken from refs. 26 and 27, respectively. All computations were performed on a DEC VAX-11/750 computer. Table 6 lists the positional co-ordinates for the non-hydrogen atoms and the bond lengths and angles are given in Table 4.

Additional material available from the Cambridge Crystallographic Data Centre comprises H-atom co-ordinates, thermal parameters, and remaining bond lengths and angles.

## Acknowledgements

We thank Jennifer S. Allen for performing some preliminary experiments, the S.E.R.C. for a studentship (to S. S. D. B.) and an allocation of time on their *X*-ray crystallographic service at Queen Mary College, Johnson Matthey Ltd. for a generous loan of gold and ruthenium salts, the Nuffield Foundation for support, Mr. R. J. Lovell for technical assistance, and Mrs. L. J. Salter for drawing the diagrams.

## References

1 Part 6, S. S. D. Brown, I. D. Salter, and L. Toupet, *J. Chem. Soc., Dalton Trans.*, 1988, 757.
2 M. Melnik and R. V. Parish, *Coord. Chem. Rev.*, 1986, **70**, 157.
3 J. J. Steggerda, J. J. Bour, and J. W. A. van der Velden, *Recl. Trav. Chim. Pays-Bas*, 1982, **101**, 164.
4 L. S. Moore, R. V. Parish, S. S. D. Brown, and I. D. Salter, *J. Chem. Soc., Dalton Trans.*, 1987, 2333; S. S. D. Brown, L. S. Moore, R. V. Parish, and I. D. Salter, *J. Chem. Soc., Chem. Commun.*, 1986, 1453.
5 M. J. Freeman, A. G. Orpen, and I. D. Salter, *J. Chem. Soc., Dalton Trans.*, 1987, 379.
6 P. A. Bates, S. S. D. Brown, A. J. Dent, M. B. Hursthouse, G. F. M. Kitchen, A. G. Orpen, I. D. Salter, and V. Šik, *J. Chem. Soc., Chem. Commun.*, 1986, 600.
7 S. S. D. Brown and I. D. Salter, *Organomet. Synth.*, in the press.
8 S. S. D. Brown, I. J. Colquhoun, W. McFarlane, M. Murray, I. D. Salter, and V. Šik, *J. Chem. Soc., Chem. Commun.*, 1986, 53.
9 R. V. Parish, in 'Mössbauer Spectroscopy Applied to Inorganic Chemistry,' ed. G. J. Long, Plenum, New York, 1984, vol. 1, p. 577.
10 S. S. D. Brown, S. Hudson, I. D. Salter, and M. McPartlin, *J. Chem. Soc., Dalton Trans.*, 1987, 1967.
11 T. Adatia, M. McPartlin, and I. D. Salter, *J. Chem. Soc., Dalton Trans.*, 1988, 751.
12 S. S. D. Brown, A. J. Dent, G. F. M. Kitchen, A. G. Orpen, and I. D. Salter, unpublished work.
13 L. J. Farrugia, M. J. Freeman, M. Green, A. G. Orpen, F. G. A. Stone, and I. D. Salter, *J. Organomet. Chem.*, 1983, **249**, 273; L. W. Bateman, M. Green, K. A. Mead, R. M. Mills, I. D. Salter, F. G. A. Stone, and P. Woodward, *J. Chem. Soc., Dalton Trans.*, 1983, 2599.
14 M. Ahlgren, T. T. Pakkanen, and I. Tahvanainen, *J. Organomet. Chem.*, 1987, **323**, 91; P. Braunstein, J. Rosé, A. Dedieu, Y. Dusausoy, J-P. Mangeot, A. Tiripicchio, and M. Tiripicchio-Camellini, *J. Chem. Soc., Dalton Trans.*, 1986, 225; B. F. G. Johnson, J. Lewis, W. J. H. Nelson, M. D. Vargas, D. Braga, K. Henrick, and M. McPartlin, *ibid.*, p. 975; J. A. Iggo, M. J. Mays, P. R. Raithby, and K. Henrick, *ibid.*, 1984, 633; B. F. G. Johnson, D. A. Kaner, J. Lewis, P. R. Raithby, and M. J. Taylor, *J. Chem. Soc., Chem. Commun.*, 1982, 314.
15 S. S. D. Brown, P. J. McCarthy, and I. D. Salter, *J. Organomet. Chem.*, 1986, **306**, C27.
16 D. F. Shriver, 'The Manipulation of Air-Sensitive Compounds,' McGraw-Hill, New York, 1969.
17 R. Uson and A. Laguna, *Organomet. Synth.*, 1986, **3**, 324.
18 R. Appel, K. Geisler, and H-F. Schöler, *Chem. Ber.*, 1979, **112**, 648.
19 W. Levason and C. A. McAuliffe, *Inorg. Synth.*, 1976, **16**, 191.
20 R. V. Parish, O. Parry, and C. A. McAuliffe, *J. Chem. Soc., Dalton Trans.*, 1981, 2098.
21 M. B. Hursthouse, R. A. Jones, K. M. A. Malik, and G. Wilkinson, *J. Am. Chem. Soc.*, 1979, **101**, 4128.
22 A. C. T. North, D. C. Phillips, and F. S. Mathews, *Acta Crystallogr., Sect. A*, 1968, **24**, 351.
23 G. M. Sheldrick, SHELX 86 Program for Crystal Structure Solution, University of Göttingen, 1986.
24 G. M. Sheldrick, SHELX 76 Program for Crystal Structure Determination and Refinement, University of Cambridge, 1976.
25 A. G. Orpen, *J. Chem. Soc., Dalton Trans.*, 1980, 2509.
26 D. T. Cromer and J. B. Mann, *Acta Crystallogr., Sect. A*, 1968, **24**, 321.
27 D. T. Cromer and D. Liberman, *J. Chem. Phys.*, 1970, **53**, 1891.

*Received* 18*th July* 1987; *Paper* 7/1530